# Correlations between the performance characteristics of a liquid crystal laser and the macroscopic material properties

S. M. Morris,* A. D. Ford, M. N. Pivnenko, O. Hadeler, and H. J. Coles†
*Centre of Molecular Materials for Photonics and Electronics, Electrical Engineering Division, Cambridge University Engineering Department, 9 JJ Thomson Avenue, Cambridge, CB3 0FA, United Kingdom*
(Received 2 August 2006; published 29 December 2006)

In order to understand how the performance of a liquid-crystal laser depends on the physical properties of the low molar mass nematic host, we have studied the energy threshold and slope efficiency of ten optically pumped liquid-crystal lasers based on different hosts. Specifically, this leads to a variation in the birefringence, the orientational order parameter, and the order parameter of the transition dipole moment of the dye. It is found that low threshold energies and high slope efficiencies correlate with high order parameters and large birefringences. To a first approximation this can be understood by considering analytical expressions for the threshold and slope efficiency, which are derived from the space-independent rate equations for a two-level system, in terms of the macroscopic liquid crystal properties.

DOI: 10.1103/PhysRevE.74.061709 PACS number(s): 42.70.Df, 42.79.Kr, 42.55.Tv, 42.70.Qs

Dye-doped chiral nematic liquid crystal (LC) lasers, which are photonic band-edge (PBE) lasers, are a potential candidate for a new generation of ultracompact coherent light sources [1–4]. This is because they exhibit features such as single-mode operation, tunability and large coherence area emission. However, for miniaturized LC lasers to become a reality the excitation threshold needs to be reduced and the slope efficiency increased. For this to happen a better understanding of the factors that influence the gain and loss terms is needed.

In a previous study we found that there was a correlation between the slope efficiency and the orientational order parameter, $S_2$ of the "local" nematic layers that constitute the chiral nematic structure [5]. This was explained by considering that $S_2$ influences the quality ($Q$) factor of the resonator cavity: the greater the local orientational order the greater the $Q$ factor. Other reports [6] have suggested that the density of photon states, $\rho$, which also determines the threshold, depends upon the birefringence. This is supported by theoretical studies carried out on PBE lasing from photonic crystal structures where it has been shown that the threshold decreases with increasing birefringence, $\Delta n$ [7–9]. This is due to a decrease in the group velocity which reduces the threshold gain. In addition, other factors unique to LC media such as the order parameter of the transition dipole moment, $S_T$, must also be considered [10].

In this paper, we present results of the input-output characteristics for ten PBE lasers based on dye-doped chiral nematic liquid crystals which have the same gain medium and active area but different nematic hosts and consequently different order parameters and birefringences. It is found that both the threshold and slope efficiency vary depending upon the nematic host that is used. In an attempt to explain these results we consider how the macroscopic physical parameters of the nematic host may influence the threshold and slope efficiency with the aid of simplified expressions derived from the space-independent rate equations for a two-level system.

For this study the ten different achiral nematic liquid crystal materials that were chosen as hosts were as follows. Five of the samples were single component achiral compounds. These five compounds were three monomesogens and two bimesogens: the three monomesogens were members from the well-known 4-cyano-4′-*n*-alkyloxybiphenyl homologous series (*n*OCB, Merck NB-C), where $n=5$, 6, and 7. The two bimesogens, synthesized in house, were the "even" nonsymmetric bimesogen $\alpha$-(2′, 4-difluorobiphenyl-4′-yloxy)-$\omega$-(4-cyanobiphenyl-4′-yloxy)octane and the "odd" nonsymmetric bimesogen $\alpha$-(2′, 4-difluorobiphenyl-4′-yloxy)-$\omega$-(4-cyanobiphenyl-4′-yloxy)nonane, herein referred to as FFO8OCB and FFO9OCB, respectively. The synthetic route for these bimesogens can be found elsewhere [11]. The remaining five materials were nematogen mixtures: BL109 (I 74 N$<$30 Cr), E7 (I 57 N$<$30 Cr), BL093 (I 93 N$<$30 Cr), E49 (I 105 N$<$30 Cr), and BL037 (I 106.5 N$<$30 Cr), (provided by Merck NB-C). Phase sequences shown in the parenthesis are in units of degree centigrade. These were chosen to increase the variation in the birefringence and order parameters and so broaden the scope of the study.

The gain medium chosen for this study was the arylidene laser dye 4-(dicyanomethylene)-2-methyl-6-(4-dimethylaminostryl)-4*H*-pyran (DCM, Lambda Physik) which is reported to have a high quantum yield and a high miscibility in liquid crystal media [4]. This laser dye, when dispersed in polar liquid crystal samples, exhibits a gain maximum at 610 nm. The gain maximum is quite broad in these samples and varies by ~1% between 600 and 620 nm [12]. As a result, the long-wavelength band edge had to be matched to 610±10 nm for each sample. This was achieved by doping each nematic LC with a low concentration of high twisting power chiral additive (2–5 wt. % depending upon the twist elastic constant of the nematic host) (BDH1281, Merck NB-C). Mixtures were capillary filled into 7.5 $\mu$m-thick cells which had rubbed polyimide alignment layers resulting in a Grandjean texture (helix axis perpen-

*Electronic address: smm56@cam.ac.uk
†Corresponding author. Electronic address: hjc37@cam.ac.uk

 ©2006 The American Physical Society

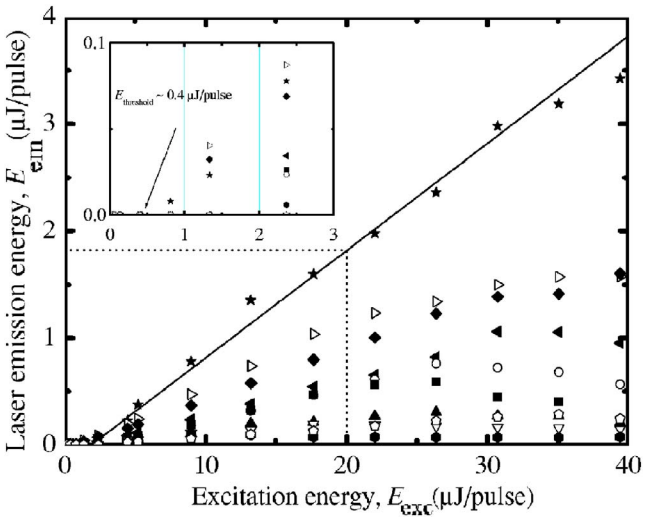


FIG. 1. (Color online) The input-output characteristics for the ten different photonic band edge lasers. The excitation source is the Nd:YAG laser ($\lambda_{exc}$=532 nm). The emission energy of the lasers, $E_{em}$, has been multiplied by a factor of two to take into account the emission in the backwards direction. The key for the figure is as follows: FFO8OCB (★), BL037 (▷), E49 (♦), BL093 (◀), 6OCB (○), 5OCB (■), 7OCB (▲), E7 (▽), FFO9OCB (⬢), BL109 (⬠).

dicular to the substrates) in the chiral nematic phase. Optical polarizing microscopy was used to confirm that a uniform distribution of the dye molecules in the LC matrix, as well as good planar alignment, had been achieved. The laser samples are denoted DCM-nematogen* where the asterisk indicates chirality.

Each sample was illuminated with focused light ($f$ =10 cm) from a frequency doubled ($\lambda$=532 nm) $Q$-switched Nd:YAG laser (Polaris II, New Wave Research). The Nd:YAG laser produced one pulse every second with a duration ($\Delta\tau_p$) of 5 ns. Both the temporal and spatial profile of the laser pulses are near Gaussian. The geometry for pumping the samples was such that the propagation vector of the irradiating light was perpendicular to the glass substrates. At the sample, the beam was focused to a circular spot with a diameter of ~100 $\mu$m. A quarter-wave plate converted the incoming linearly polarized light into circularly polarized light of the opposite rotation sense of the helix prior to the sample so as to maximize the penetration depth of the pump light. Samples were mounted on a custom built heating stage (Linkam) that was fixed to a translation stage built in house. A controller was used to regulate the temperature of the sample (TMS94, Linkam) to a stability of 0.1 °C. In both cases, the emission from the sample was collected in the forward direction (parallel to the normal of the cell walls) over a narrow solid angle by a microscope objective and directed onto a free-space energy detector (PD10 silicon photodiode head and Laserstar energy meter, Ophir). A removable beam splitter enabled the wavelength of the laser beam to be monitored during measurements by an optical fiber/USB-based spectrometer. The birefringence of each sample was determined at a wavelength of $\lambda$=589.8 nm using an Abbé refractometer.

TABLE I. The lasing thresholds ($\mu$J/pulse) and slope efficiencies (%) for the ten photonic band edge laser samples (DCM-nematogen*). The table has been arranged in ascending order of the lasing threshold.

| Material | Temperature (°C) | Excitation threshold, $E_{th}$ ($\mu$J/pulse) | Slope efficiency, $\eta_s$ (%) |
|---|---|---|---|
| DCM-FFO8OCB* | 95 | 0.4 | 12 |
| DCM-BL037* | 30 | 0.8 | 6 |
| DCM-E49* | 30 | 0.8 | 5 |
| DCM-BL093* | 30 | 1.3 | 3 |
| DCM-6OCB* | 43 | 1.3 | 3 |
| DCM-5OCB* | 35 | 1.3 | 3 |
| DCM-FFO9OCB* | 75 | 1.3 | 2 |
| DCM-BL109* | 30 | 1.3 | 2 |
| DCM-7OCB* | 45 | 2.4 | 1 |
| DCM-E7* | 30 | 2.4 | 1 |

The input-output characteristics of each LC laser are plotted in Fig. 1. The datum represents the sum of the forward and backward emissions from the LC cavity. All the lasers emit at a wavelength of 610±10 nm (within the gain maximum). The inset of the figure represents the input-output characteristics magnified near to the excitation thresholds. For each plot the excitation threshold occurs below an excitation energy of 3 $\mu$J/pulse. Above the excitation threshold the emission energy increases linearly with excitation energy. For excitation energies greater than 10 $\mu$J/pulse, the emission energy for several of the laser samples reaches saturation, namely DCM-FFO9OCB*, DCM-E7*, and DCM-7OCB*. Saturation of the laser output for the remaining samples occurs between 20 and 25 $\mu$J/pulse with the exception of sample DCM-FFO8OCB* which did not reach saturation until an input of 40 $\mu$J/pulse.

In Table I, the excitation thresholds, $E_{th}$, and the slope efficiencies, $\eta_s$ are given at the laser's lowest operating temperature. It is shown that the laser sample DCM-FFO8OCB* has both the lowest excitation threshold ($E_{th}$=0.4 $\mu$J/pulse) and the highest slope efficiency (12%) whereas at the other end of the scale the laser samples DCM-E7* ($E_{th}$=2.4 $\mu$J/pulse, $\eta_s$=1%) and DCM-7OCB*, ($E_{th}$=2.4 $\mu$J/pulse, $\eta_s$=1%) have excitation thresholds that are six times that of DCM-FFO8OCB*.

To understand these results, albeit qualitatively, we consider the space-independent rate equations for a two-level system. For our experiment, pumping was in the form of optical pulses with duration, $\Delta\tau_p$, of 5 ns. This is long enough for a population inversion to occur but less than the time required for a population of the triplet manifold of the laser dye. Therefore, we assume a quasisteady-state condition whereby the rate of change of the number of photons in the cavity mode ($dq/dt$) and the rate of change of the excited state population ($dN_1/dt$) are both zero and ignore intersystem crossing. From the space-independent rate equations for a two-level system, $dq/dt$ and $dN_1/dt$ can be expressed as [13]

$$\frac{dq}{dt} = W_L N_1 q - \Gamma q = 0, \tag{1}$$

and

$$\frac{dN_1}{dt} = R_p - qW_L N_1 - \frac{N_1}{\tau} = 0, \tag{2}$$

respectively, where $W_L$ is the stimulated emission rate, $\Gamma$ represents the losses, $R_p$ is the pump rate, and $\tau$ is the excited state lifetime (including both radiative and nonradiative terms). In this study, we are primarily interested in the energies of the laser field and hence the photon number $q$ is related to the energy density, $E' : E' = h\nu\langle q\rangle / V$ where $V$ is the modal volume. In accordance, the population density is then $n_1 = N_1 / V$.

In order to simplify the analysis further, we assume homogeneous pumping: the pump rate is then given by $R_p = F \cdot N_0 \cdot \sigma_a$, where $F$ is the flux, $N_0$ is the population in the ground state, and $\sigma_a$ is the absorption cross section. The flux is related to the power, $P$, by $F = P / Ah\nu_p$, where $A$ is the pump area and $h\nu_p$ is the energy of the pump photons. For our experiments the average power is the average energy contained within the pulse duration i.e., $P = E_{\text{exc}} / \Delta\tau_p$. By inserting the relationship for the flux, and consequently power, into $R_p$ and then rearranging for $E_{\text{exc}}$ we get

$$E_{exc} = R_p \left( \frac{h\nu_p}{N_0 \sigma_a} \right) A \Delta\tau_p. \tag{3}$$

By replacing $R_p$ with $\Gamma / W_L \tau$ [from the space-independent rate equations (1) and (2)] and setting the excitation energy to the threshold, an expression for the energy threshold can then be obtained

$$E_{th} = \frac{Ah\nu_p}{N_0 \sigma_a} \left( \frac{\Gamma}{W_L} \right) \left( \frac{\Delta\tau_p}{\tau} \right). \tag{4}$$

Here we assume that $\sigma_a$ remains constant for DCM in the host materials due to the fact that the chemical structures of the hosts are very similar. This relationship suggests that the excitation threshold is increased if the pump-pulse duration is increased. Experimentally, Cao *et al.* have found that $E_{\text{th}}$ does indeed increase when the pump pulse duration is increased from a picosecond to a nanosecond time scale [14].

For the slope efficiency, which can be defined as $\eta_s = dE_{out} / dE_{exc}$, the analytical solutions to the rate-equations for a two-level system, in combination with the expression for the energy threshold given in Eq. (4), results in

$$\eta_s = \frac{N_0 \sigma_a d}{h\nu_p \Gamma \Delta\tau_p}, \tag{5}$$

where $d$ is the thickness of the medium.

Although these relationships result from a number of simplifying assumptions for the kinetic behavior of the liquid crystal lasers they do relate several parameters which are of fundamental importance for LC lasing, namely: the stimulated emission rate, $W_L$, and the loss mechanisms, $\Gamma$. First, let us consider the stimulated emission rate, $W_L$.

The single most important aspect that determines which band edge has the lower lasing threshold, provided that the gain is equal at both edges, is the orientation of the transition dipole moment of the dye with respect to the director. This depends upon the molecular shape of the dye and the orientation of the transition dipole moment with respect to its long axis. The theoretical work of Schmidtke and Stille [10] has shown that the rate of spontaneous emission of the dye into each of the resonant modes in the weak coupling regime depends upon the projection of the electric field vector at the band edge, $e$, on the transition dipole moment of the dye, $\mu$. This in turn is directly proportional to the order parameter of the transition dipole moment, $S_{\text{T}}$. Positive values of $S_{\text{T}}$ indicate that the emission is predominantly into the mode situated at the long-wavelength edge whereas negative values favour the short-wavelength edge.

Since the spontaneous emission rate is a function of $S_T$ it is reasonable to assume that the stimulated emission rate $W_L$ also depends on $S_T$. Therefore, a larger absolute value of $S_T$ will result in a larger $W_L$ and consequently a lower threshold. We therefore consider the stimulated emission rate in the form $W_L = f(S_T)$.

For the loss term, $\Gamma$, we consider that at the threshold the loss and gain terms are equal, i.e., $\Gamma = g_{\text{th}}$. In this case the LC laser may be considered as a type of distributed feedback laser (DFB) and based on coupled-mode theory Kogelnik and Shank derived an expression for the threshold gain for the weak-coupling regime [15]

$$g_{th} = \frac{\lambda^2}{\Delta n^2 d^3}. \tag{6}$$

Taking the simplest possible model, the birefringence, $\Delta n$, at a specific temperature can be written in terms of the orientational order parameter, $S_2$, and a term that represents the molecular polarizability anisotropy, e.g., $\Delta n = \Delta n_0 S_2$ where $\Delta n_0$ is the birefringence extrapolated to zero Kelvin. Replacing $\Delta n$ with $\Delta n_0 S_2$ in the expression for the threshold gain (6), and then substituting this into (4) and (5) we get

$$E_{th} \propto \frac{Ah\nu_p}{N_0 \sigma_a} \left( \frac{\Delta\tau_p}{\tau} \right) \left( \frac{1}{W_l(S_T)} \right) \left( \frac{\lambda^2}{\Delta n_0^2 S_2^2 d^3} \right) \tag{7}$$

and

$$\eta_s \propto \left( \frac{N_0 \sigma_a d}{h\nu_p \Delta\tau_p} \right) \left( \frac{\Delta n_0^2 S_2^2 d^3}{\lambda^2} \right), \tag{8}$$

respectively. Note that the dependence of $E_{\text{th}}$ on the cell thickness, $d$, is different to that obtained by Cao and Palffy-Muhoray [14] because in this case we have neglected losses related to absorption.

The three LC parameters ($\Delta n_0$, $S_2$, and $S_T$) that appear in the expressions for the threshold and the slope efficiency are given for each sample in Table II. To compare the different LC lasers we introduce two figure-of-merit (FOM) parameters: one for threshold, $f_{\text{threshold}}$, and one to represent the slope efficiency, $f_{\text{efficiency}}$. These are subsequently defined as $f_{\text{threshold}} = {\Delta n_0}^2 \cdot {S_2}^2 \cdot S_T \cdot 100$ and $f_{\text{efficiency}} = {\Delta n_0}^2 \cdot {S_2}^2 \cdot 100$, respectively. The excitation threshold and slope efficiency are plotted as a function of the corresponding FOM parameters in Fig. 2. Although there is significant scatter in the data, two trends are clearly identified. That is, large values for $f_{\text{threshold}}$

TABLE II. Values for the three key parameters: birefringence at zero Kelvin ($\Delta n_0$) and the orientational order parameter ($S_2$) associated with the pseudo-nematic layers, which were determined from Haller-type fits to the birefringence. The order parameter of the transition dipole moment ($S_T$) of the dye calculated from absorbance measurements. In addition, the birefringence of the sample at the laser operating temperature is also provided in the first column ($\Delta n = \Delta n_0 S_2$).

| Host Material | $\Delta n$ | $\Delta n_0$ | $S_2$ | $S_T$ |
|---|---|---|---|---|
| FFO8OCB | 0.26 | 0.35 | 0.73 | 0.48 |
| BL037 | 0.27 | 0.39 | 0.69 | 0.40 |
| E49 | 0.26 | 0.40 | 0.65 | 0.37 |
| 6OCB | 0.21 | 0.38 | 0.56 | 0.33 |
| BL093 | 0.24 | 0.37 | 0.62 | 0.28 |
| 5OCB | 0.21 | 0.38 | 0.56 | 0.34 |
| FFO9OCB | 0.20 | 0.31 | 0.64 | 0.42 |
| BL109 | 0.18 | 0.31 | 0.56 | 0.34 |
| 7OCB | 0.19 | 0.33 | 0.57 | 0.34 |
| E7 | 0.20 | 0.36 | 0.56 | 0.35 |

result in low threshold energies and large values for $f_{\text{efficiency}}$ result in high slope efficiencies. These results are in agreement with the fact that a higher $\rho$ (due to a higher $\Delta n$) results in a lower $E_{\text{th}}$ and a higher $\eta_s$.

The exception to this rule is DCM-FFO8OCB* which has a lower value for $f_{\text{efficiency}}$ than DCM-BL037* yet it exhibits a much higher slope efficiency. Therefore, in this case the magnitude of the birefringence and order parameters do not correlate with the corresponding slope efficiency. Furthermore, this suggests that the slope efficiency does not depend solely upon the density of photon states, $\rho$, at the band edge. As a result, other physical parameters must also be of importance. One set of physical parameters that are significantly different for the FFO8OCB compound compared with the remaining nematic hosts are the elastic constants, which are almost a factor of two greater than those of the monomesogens and the odd-spaced bimesogen FFO9OCB. For a Fabry-Perot laser the slope efficiency depends upon the saturation intensity which is related to additional loss mechanisms. It is known that large elastic constants result in reduced scattering from director fluctuations and this would then lead to reduced scattering losses from the laser cavity and consequently higher saturation intensity. This is in accord with the higher saturation limit observed for the DCM-FFO8OCB* laser compared with the other laser samples (c.f., Fig. 1). Further studies are being conducted to understand the higher slope efficiency of DCM-FFO8OCB*.

This caveat aside, these findings suggest that in general, low thresholds and high slope efficiencies correlate with a combination of high molecular polarizability ($\Delta n_0$), high orientational order parameter ($S_2$), and high order parameter of the transition dipole moment ($S_T$). The bimesogen hosts, which have a degree of flexibility, enable a good alignment between the dye and the host. However, the host must also adopt a packing configuration such that the macroscopic optical and order parameters are enhanced; this is not the case for the odd-spaced bimesogen, FFO9OCB.

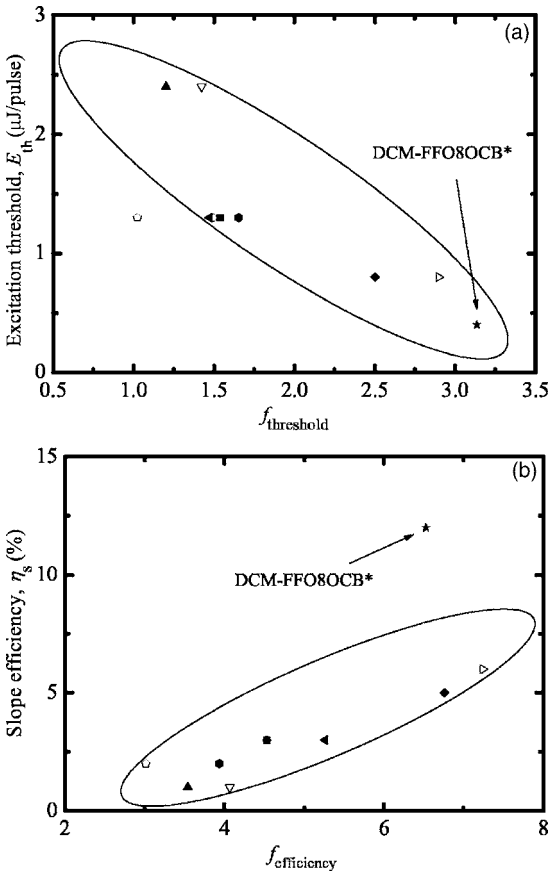


FIG. 2. (a) The excitation threshold as a function of the figure-of-merit parameter, $f_{\text{threshold}}$, ($f_{\text{threshold}} = \Delta n_0^2 \cdot S_2^2 \cdot S_T \cdot 100$) and (b) the slope efficiency as a function of the figure-of-merit parameter, $f_{\text{efficiency}}$, ($f_{\text{efficiency}} = \Delta n_0^2 \cdot S_2^2 \cdot 100$). The key for the figure is as follows: FFO8OCB (★), BL037 (▷), E49 (◆), BL093 (◀), 6OCB (○), 5OCB (■), 7OCB (▲), E7 (▽), FFO9OCB (⬢), BL109 (⬠).

In this work, we have been concerned with the correlation between the performance of a LC-based photonic band edge laser and the macroscopic properties of the nematogen host. It was found that the threshold (slope efficiency) is inversely (directly) proportional to functions of the order parameters, $S_2$ and $S_T$ as well as the birefringence at zero Kelvin, which is an indication of the molecular polarizability. This is in agreement with the concept that $E_{\text{th}} \propto 1/\rho$ and $\eta_s \propto \rho$. Measurements of the input-output characteristics showed that, on average, liquid crystals which combine higher order parameters with larger birefringences do tend to exhibit lower threshold energies and higher slope efficiencies, in accord with a larger density of photon states at the band edge. However, one anomaly was observed in the slope efficiency which suggests that other factors, in addition to those that influence the density of photon states, must also be considered.

The authors wish to thank Merck NB-C for kindly supplying the monomesogens, the chiral dopant, and the nematogen mixtures. The bimesogens were synthesized in house by Dr. Andrew Blatch. A.D.F. acknowledges EPSRC and Dow Corning for their support through the COMIT Faraday Partnership.

[1] J. P. Dowling, M. Scalora, M. J. Bloemer, and C. M. Bowden, J. Appl. Phys. **75**(4), 1896 (1994).
[2] V. I. Kopp, Z.-Q. Zhang, and A. Z. Genack, Phys. Rev. Lett. **86**(9), 1753 (2001).
[3] V. I. Kopp, B. Fan, H. K. M. Vithana, and A. Z. Genack, Opt. Lett. **23**(21), 1707 (1998).
[4] B. Taheri, P. Palffy-Muhoray, and H. Kabir, *ALCOM Symposium. Chiral Materials and Applications*, Cuyahoga Falls, Feb. 18–19 (1999); B. Taheri, A. Munoz, P. Palffy-Muhoray, and R. Twieg, Mol. Cryst. Liq. Cryst. Sci. Technol., Sect. A **358**, 73 (2001).
[5] S. M. Morris, A. D. Ford, M. N. Pivnenko, and H. J. Coles, J. Appl. Phys. **97**, 023103 (2005).
[6] K. L. Woon, M. O'Neill, G. J. Richards, M. P. Aldred, and S. M. Kelly, Phys. Rev. E **71**, 041706 (2005).
[7] K. Sakoda, Opt. Express **4**, 167 (1999).
[8] N. Susa, J. Appl. Phys. **89**, 815 (2001).
[9] S. Nojima, J. Appl. Phys. **90**, 545 (2001).
[10] J. Schmidtke and W. Stille, Eur. Phys. J. B **31**, 179 (2003).
[11] H. J. Coles, M. J. Coles, S. P. Perkins, B. M. Musgrave, and D. Coates, *Bimesogenic Compounds and Their Use in Flexoelectric Devices*, EU patent, EP99119114 (1999).
[12] Y. Huang, Y. Zhou, and S.-T. Wu, Appl. Phys. Lett. **88**, 011107 (2006).
[13] O. Svelto, *Principles of Lasers*, 4th edition (Plenum Press, New York, 1998).
[14] W. Cao, P. Palffy-Muhoray, B. Taheri, A. Marino, and G. Abbate, Mol. Cryst. Liq. Cryst. **429**, 101 (2005).
[15] H. Kogelnik and C. V. Shank, J. Appl. Phys. **43**, 2327 (1972).